Sensor-Driven Musculoskeletal Dynamic Modeling*

Laura A. Hallock[1], Robert Peter Matthew[1], Sarah Seko[1] and Ruzena Bajcsy[1]

Abstract— **The creation of a descriptive human dynamical model useful in upper-limb prosthesis and exoskeleton control remains an open problem. We here present a framework that approaches model generation from a "sensor-driven" design perspective that explicitly avoids over-fitting parameters and minimally relies on literature values and biological assumptions. We further apply this framework to a simplified dynamical model of the human elbow and verify using synthetic data that the problem of fitting this model to a real system is well-posed. Lastly, we apply the same simplified model to real surface electromyography (sEMG) and contact force data of a single subject. While the dynamical model extracted from this data is biologically nonsensical, the results indicate that this framework represents a viable starting point from which to build more sophisticated fully-recoverable dynamical models.**

I. Introduction

A. Motivation

A major obstacle to the creation of effective prosthetic and exoskeletal devices is our inability to model the dynamical properties of the system: while a designer can often precisely characterize the device they create, they are forced to rely on peripheral signals like surface electromyography (sEMG) — or resort to extremely invasive techniques — to model the underlying dynamics of the human user. This inference problem (from peripheral signals to dynamics) is difficult for the following reasons:

- The human musculoskeletal system is (computationally intractably) complex. (The elbow joint, for example — as a hinge, arguably the simplest joint in the body — is actuated by eight different muscle groups, each of which exhibits highly nonlinear dynamics.) Even the force-length-velocity relation of a single muscle is inadequately understood.
- Peripheral signals (e.g., sEMG) are often unable to provide any information about deep muscle groups, so information can only be gathered from surface muscles.
- Muscle/tendon models are often based on literature values and population measures that vary widely from subject to subject. These models are especially inadequate because the target patient group for exoskeleton and prosthesis use (e.g., spinal cord injury survivors, amputees, muscular dystrophy patients) have musculoskeletal morphology that is by definition pathological and therefore poorly served by these models.

*This work was supported by the Berkeley Vision and Learning Center.

[1]L. A. Hallock, R. P. Matthew, S. Seko, and R. Bajcsy are in the department of electrical engineering and computer science at UC Berkeley, USA { lhallock, rpmatthew, seko, bajcsy } @eecs.berkeley.edu

Despite these challenges, modeling the dynamics of the human body is integral to the development of exoskeleton and prosthesis control systems. While peripheral sensing (e.g., motion capture) can largely recover human kinematics, understanding contact forces — for instance, identifying whether the user is lifting a feather or a barbell — is essential if we hope to replicate human manipulation and locomotion abilities.

B. Related Work

Current human dynamical models are often built on an amalgamation of literature values and assumptions drawn from cadaver and *ex vivo* studies (both human and animal) and from population measures (e.g., average limb-mass-to-total-mass ratio). These measures have been aggregated into several "average human" modeling frameworks, including OpenSim [1] and AnyBody [2]; while these frameworks can often be grossly customized to an individual, they cannot accommodate significant musculoskeletal pathologies and rely on many hidden assumptions of morphological parameters.

For specific, well-defined tasks, additional assumptions can be made to formulate optimization cost functions that allow for model fitting (e.g., when examining human walking, requiring the model to match a reasonable human gait cycle or assuming that self-selected walking speed is metabolically optimal). While these types of assumptions have allowed for the creation of descriptive lower-limb dynamical models [3], such cost functions are often much more difficult to formulate for upper-limb manipulation tasks.

II. Objectives

The ultimate goal of this research is to create a musculoskeletal model of the human arm with the following characteristics:

Appropriate level of abstraction. The model is as simple as possible while accurately predicting the kinematics and dynamics of each limb segment (upper limb, lower arm, and hand) when appropriately trained to an individual and accommodates highly pathological muscle morphologies.

Trainable/customizable using non-invasive sensing. The model can be made subject-specific using non-invasive sensing technologies. This customization step may include both directly observing morphological parameters (e.g., using ultrasound, MRI) and acquiring a dataset on which to perform more traditional machine learning (e.g., using sEMG, near-infrared spectrophotometry (NIRS), motion capture).

Runnable (predictive) using non-invasive, wearable sensing. Once the model is customized to a given individual,

it should dynamically predict the kinematics and dynamics of the individual while relying only on portable, non-invasive sensing (e.g., using sEMG, inertial measurement units (IMU), NIRS). This is arguably the most difficult constraint to satisfy but is essential if the model is to be useful in the context of a prosthetic device.

Non-reliant on literature values or population measures. The model may rely on literature-informed structural assumptions (e.g., the general form of the muscle force-length-velocity relation), but any parameters are fitted to the individual through data collection, not drawn from literature values.

The approach described in this paper represents a first step toward the creation of such a model.

A. Assumptions

In model creation, we assume the ability to measure

- *skeletal kinematics*, including joint positions / velocities / accelerations (via motion capture, IMU, electrogoniometer, etc.);
- *morphological parameters*, including muscle / tendon / bone volumes / insertion points (via ultrasound, MRI, etc.) and limb link masses (via method proposed in [4]);
- *contact forces* of both support contacts and end effectors (via force plates, force-torque sensors, etc.);
- *dimensionless muscle "activation"*, in aggregate (via sEMG); and
- *peripheral signals*, such as blood oxygenation (via NIRS, pulse oximetry, etc.) and metabolic effort (via oxygen consumption mask, etc.).

Although measuring many of the parameters listed above in a reliable, automated way is an open problem, our modeling framework is designed to accommodate the degree of reliability we can expect from the above sensors.

B. Approach

Based on the above objectives and available sensing modalities, we have chosen to employ a "sensor-driven" design paradigm: our modeling framework is informed by both *a)* sensor capability and *b)* the kinematic and dynamic parameters of interest. The goal of this project is *not* to create the most biologically-correct model of the human arm possible: instead, we hope to create a model that accurately and descriptively predicts the kinematics and dynamics of an individual in a manner that allows for safe and useful interaction with exoskeletons, prostheses, and other robotic devices. Thus, we choose to approach the problem from a systems-engineering, optimization, and modeling perspective rather than a biological one.

III. Simplified Model

As an initial proof-of-concept, we seek to formulate the simplest possible model that can be experimentally validated. We thus consider the elbow in isolation, in the two-dimensional sagittal plane, as a frictionless hinge joint actuated by a single, massless flexor muscle that spans the joint (shown in Fig. 1). The upper arm is assumed perpendicular to the ground, and the lower arm's mass is assumed concentrated as a point mass at the extremal end of the lower link.

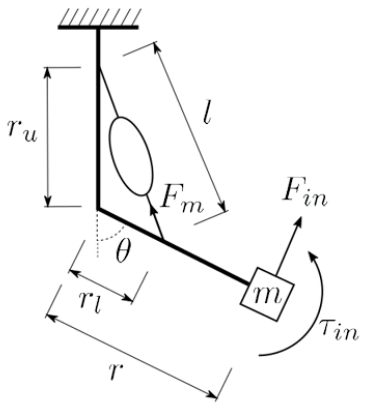

Fig. 1: Simplified human elbow model. Parameters described in detail in section III.

A. Parametrization

We assume that the force-length relation of the single muscle is described by the relation

$$F_m(\bar{l}) = F_0(\beta_1 \bar{l}^2 + \beta_2 \bar{l} + \beta_3) \tag{1}$$

for some unknown parameters β_i, $i \in \{1, 2, 3\}$, where $\bar{l} = \frac{l}{l_{opt}}$ is the length of the muscle, normalized by the optimal operating length l_{opt}, and F_0 is the maximum isometric muscle fiber force.

Note that we examine this system, for simplicity, only under static conditions; otherwise, the muscle force relation above would also include a dependence on velocity.

We further assume that this force relation is scaled linearly by a measure of "activation", $\bar{a} = \frac{a}{a_{max}}$, that can be extracted from sEMG signals. The dynamic equation of the system can thus be written as

$$\begin{aligned} \tau &= \tau_{in} + rF_{in} - \frac{1}{2}mgr\sin\theta \\ &= F_0 r_l r_u \bar{a} \sin\theta [\frac{l}{l_{opt}^2}\beta_1 + \frac{1}{l_{opt}}\beta_2 + \frac{1}{l}\beta_3] \end{aligned} \tag{2}$$

for total end effector torque τ, joint angle θ, radius r, muscle attachment points r_l and r_u, and gravitational constant g.

B. Model Validation

To evaluate this model's viability, we sought to determine whether, given known values F_0, r_l, r_u, and l_{opt}, as well as a data series of n tuples $(\bar{a}_j, \tau_j, \theta_j)$, $j \in \{1, ..., n\}$, we could recover muscle force-length parameters β_i. This validation was performed in several steps, as detailed below: first, we assumed biologically reasonable values for β_i and swept through a range of τ and θ values to generate artificial $\bar{a}$ values; second, ignoring these assumed β_i values, we added noise to each data series, aggregated the data into a regression matrix, and performed least squares optimization to recover

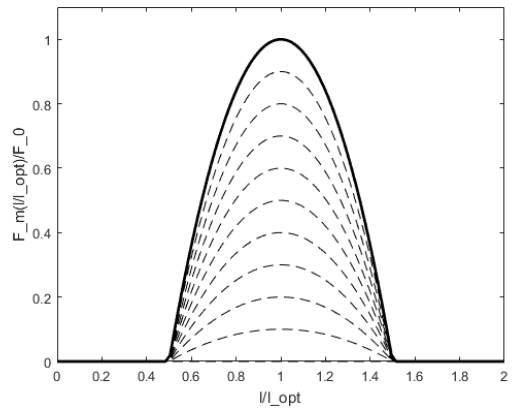

Fig. 2: Quadratically-approximated, normalized force-length relation. Bold data line shows maximally-activated muscle, such that maximal muscle force occurs at optimal muscle length and maximal activation. Dashed lines show submaximally activated force-length relations.

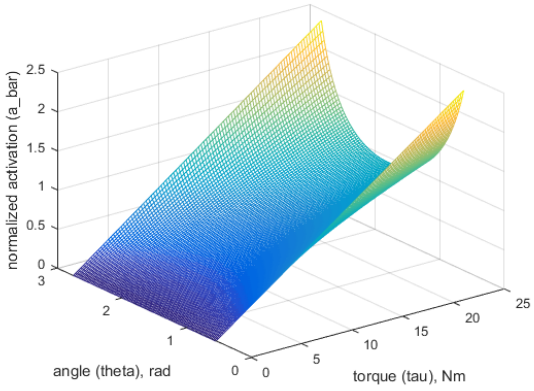

Fig. 3: Generated $(\bar{a}, \tau, \theta)$ surface. Expected activation increases with greater torque output τ and with θ values that result in muscle length that is farther from optimal.

fitted β_i; third, we performed this optimization over a range of noise magnitudes and observed both the condition number of the regression matrix and the deviation of each β_i from the value that generated the synthetic data.

1) Synthetic Data Generation: To generate synthetic data, we chose parameters $\beta_1 = -4$, $\beta_2 = 8$, and $\beta_3 = -3$, in an approximation of the muscle force-length relationship described by [5] and employed by [6] (shown in Fig. 2). Additionally, to approximate the biceps muscle — and to mirror as closely as possible the experimental validation described in section IV — we chose morphological parameters $r_l = 0.05$m, $r_u = 0.3$m, $l_{opt} = 0.3$m, and $F_0 = 500$N. To approximate a normal operating range, we swept through values $\tau \in [0, 24.5]$N and $\theta \in [0.55, 2.75]$rad. The recovered $(\bar{a}, \tau, \theta)$ surface is shown in Fig. 3.

2) Model Recovery: We then added various levels of white Gaussian noise to each $(\bar{a}_j, \tau_j, \theta_j)$ data series and

SNR (dB)	cond(W)	$\sum_{i=1}^{3} \frac{\lvert\beta_i - \beta_i^{fit}\rvert}{\lvert\beta_i\rvert}$
100	591.0	0
10	624.2	0.0248
1	619.1	0.0472
1e-2	625.7	0.0309
1e-64	622.3	0.0341

TABLE I: Condition number of W and error of B for various signal-to-noise ratios. SNR values reflect the $\bar{a}$, τ, θ (i.e., the same level of white Gaussian noise was added to each data series). Condition numbers and error remain similar for varying levels of noise.

aggregated the data into dynamics relation

$$\begin{bmatrix} \tau_1 \\ \vdots \\ \tau_n \end{bmatrix} = F_0 r_l r_u \begin{bmatrix} \frac{l_1}{l_{opt}^2} \sin\theta_1 \bar{a}_1 & \frac{1}{l_{opt}} \sin\theta_1 \bar{a}_1 & \frac{1}{l_1} \sin\theta_1 \bar{a}_1 \\ \vdots & \vdots & \vdots \\ \frac{l_n}{l_{opt}^2} \sin\theta_n \bar{a}_n & \frac{1}{l_{opt}} \sin\theta_n \bar{a}_n & \frac{1}{l_n} \sin\theta \bar{a}_n \end{bmatrix} \begin{bmatrix} \beta_1 \\ \beta_2 \\ \beta_3 \end{bmatrix}$$

or, more succinctly,

$$T = WB \tag{3}$$

for τ data vector T, regression data matrix W, and parameter vector B. We then solved the unconstrained least squares optimization problem

$$\min_B \parallel T - WB \parallel_2^2 \tag{4}$$

using MATLAB's CVX library ([7], [8]) to recover parameter vector B.

3) Preliminary Sensitivity Analysis: To verify this optimization's validity, we confirmed that the recovered B values were similar to those of the B vector used to obtain the synthetic data. Additionally, we examined the condition number of W — as a measure of how "close" the matrix was to singular — and performed a numerical computation of base parameters (as described in [9]) to ensure that the parameters were not interdependent in ways that made them unrecoverable.

As summarized in Table I, recovered B values were all with 5% of the generative B, even with the addition of nontrivial white Gaussian noise to each data series. Additionally, while the condition numbers of W are somewhat high, both they and the numerical computation of base parameters indicate that we can, in fact, expect to recover the entire parameter vector B. We thus conclude that our model is stable to perturbations in each data series $\bar{a}$, τ, and θ and is thus a good starting point from which to build more sophisticated models.

IV. Experimental Validation

In addition to our evaluation using synthetic data, we tested the modeling framework using sEMG, kinematic, and contact force data from a single subject, as detailed below.

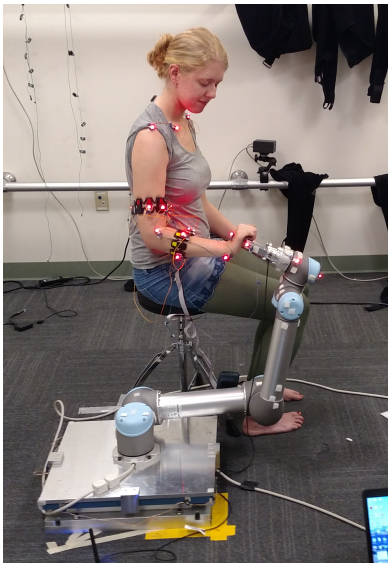

Fig. 4: Experimental setup. For this experiment, data were analyzed only from a single channel on the Myo on the upper arm and the force-torque sensor mounted to the UR5 robot. Additionally, note that subject's forearm was fully supinated during data collection, unlike the pose shown in this image.

A. Sensors and Equipment

To acquire subject-specific EMG, kinematic, and force output data, the following sensors and equipment were used:

Myo sEMG armband. The Myo is a commercial armband produced by Thalmic Labs, Inc. and marketed for interacting with computers and other devices using gesture recognition (e.g., during a presentation). The developer SDK allows for Bluetooth access to eight channels of raw EMG data at 200 Hz; in this experiment, we used a single channel positioned near the subject's biceps.

Force-torque sensing. To measure the subject's applied forces and torques, we used the Mini45 Force/Torque Sensor produced by ATI Industrial Automation. This six-degree-of-freedom sensor simultaneously measures three force components (F_x, F_y, F_z) and three torque components (τ_x, τ_y, τ_z) along orthogonal directions by using silicon strain gauges to convert the applied load into forces and torques.

Video recording. The subject's elbow joint angle was manually extracted from still images of the experiment. In the future, more sophisticated motion capture systems (e.g., PhaseSpace) will be used to more accurately extract kinematic and dynamic parameters of interest.

B. Setup

A Myo armband was positioned on the subject's upper arm (Fig. 4). All data were collected in a single session to keep the Myo position invariant, as small changes in electrode location can impact the sEMG signal.

Each experimental trial consisted of a subject repeatedly pressing on a handle mounted to a force sensor. During the experiment, a visual display instructed the subject to press with a force level of "light", "medium", or "hard" for a duration of 2s with a 1s break between each press. A trial consisted of 21 presses with randomized force levels.

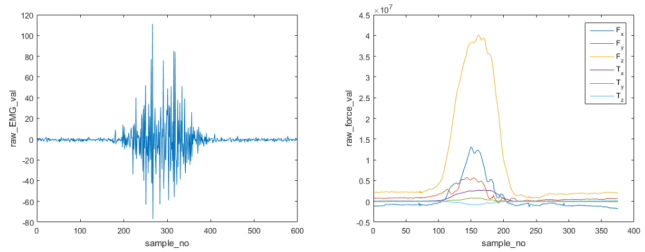

Fig. 5: An example segmented data point. *Left*: Raw sEMG data. *Right*: Raw force-torque data. Angle values were extracted from still images of the experimental setup.

To allow for force-torque sensor placement in multiple locations relative to the user, the sensor was mounted to a manually-configured UR5 robot arm. The arm position was kept within a plane such that the upper arm remained perpendicular to the ground and the forearm remained aligned within the natural sagittal plane. During each trial, the subject was instructed to keep her wrist completely supinated. Data were collected in a total of 7 kinematic configurations. At each configuration, a trial consisting of 21 presses was conducted.

C. Data Segmentation

In post-processing, the data were segmented into 3s samples, each of which corresponded to a single press (2s) and rest (1s). Each of these segmented data points then formed the basis for a $(\bar{a}, \tau, \theta)$ data point: $\bar{a}$ was taken as the maximum value over the absolute value of the EMG signal smoothed by a first-order Butterworth filter and normalized by the maximum activation recorded at any data point; F_{in} was taken as the sum of the absolute value of the maximum of F_x and F_z as recorded by the force-torque sensor and used to generate τ using Eq. 2; θ was manually measured from camera recordings of the experimental setup. An example data point is shown in Fig. 5.

The same morphological parameters enumerated in section III-B.1 were used, in addition to $r = 0.35$m, $m = 1$kg, and $g = 9.8$m/s^2. Length measurements were taken from rough measurements of the subject; the mass measurement was computed using the biomechanical scaling tables in [10].

D. Model Fitting

As described in section III-B.2, the $(\bar{a}, \tau, \theta)$ points were aggregated into vector T and matrix W, and the same least squares optimization was performed to extract B.

E. Preliminary Results

As in section III-B.3, both the condition number of W (662.6) and the numerical computation of base parameters indicate that least squares should be able to extract the full B vector. As shown in Fig. 6, the $(\bar{a}, \tau, \theta)$ plane fitted to the data by the optimization is qualitatively reasonable: a larger activation value is expected during higher torque output and

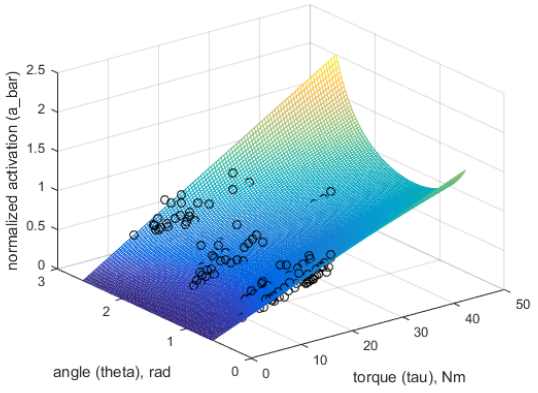

Fig. 6: Fitted $(\bar{a}, \tau, \theta)$ surface. The surface is qualitatively similar to the synthetically generated surface in Fig. 3 and fits the data well.

when muscle length is farther from optimal, and this is reflected in the fitted plane. The extracted B vector, however — $\beta_1 = 2.2767$, $\beta_2 = 0.6201$, and $\beta_3 = -0.5573$ — is biologically nonsensical: in fact, it implies that the muscle force-length relation $F_m(\bar{l})$ (shown in Eq. 1) is a convex quadratic, implying that muscle force decreases at the same activation as muscle length nears l_{opt}, the opposite of the expected relation. The fact that a function so qualitatively different from the predicted, concave $F_m(\bar{l})$ can still accurately predict $(\bar{a}, \tau, \theta)$ data in a reasonable way means that more investigation is required to determine the relationship between the generated B and the fitted surface, including what additional parameters may need to be measured to ensure a biologically reasonable fit.

V. Conclusions

We have here presented a model of the human elbow that, while vastly simplified, represents the first step toward a descriptive dynamical model of the human arm. While we did not see biologically reasonable results from our preliminary experiments, our tests indicate that the model is indeed experimentally verifiable and has the potential to unify contact force data with internal human dynamics.

VI. Future Work

This project is ongoing, and we hope to further refine and develop this model in the following ways:

Incorporate better, more extensive data. When performing data collection, we noticed a number of potentially confounding factors, including sensor placement and morphological measurement accuracy. In the future, we hope to take more data in which sEMG sensors are more precisely placed and morphological parameters are more precisely measured (e.g., using ultrasound or MRI). Additionally, because forces were exerted by the subject's hand, the total force exertion may not have been directly reflected as elbow torque, as some is required to maintain wrist stiffness. In future experiments, subjects will be asked to wear a wrist brace to mitigate this confounding factor. Lastly, this experiment employed only a single channel of sEMG: in the future, we hope to employ more, redundant sEMG channels to help account for signal noise.

Incorporate multiple muscles and additional dimensions. Each joint in the human body is actuated by multiple muscles; in the future, we hope to extend this single-muscle model to include both extensors and additional flexors. Additionally, we hope to expand the model to include additional joints degrees of freedom, both within and outside the sagittal plane.

Hybridize model. Studies suggest that muscles operate with different force-length-velocity relations when they perform as the agonist versus the antagonist in a given motion; thus, the human model of the arm lends itself to hybridization.

Add dynamics. The model presented here is purely static; we hope to extend this model to explicitly operate in dynamic regimes.

Acknowledgment

I thank Robert Peter Matthew for significantly aiding in project formulation and execution, as well as data collection; Sarah Seko, for aid in data collection and processing; Prof. Ruzena Bajcsy, for providing general project insight and equipment; and Prof. Claire Tomlin, for providing general project advice.

References

[1] Delp, S.L. et al. "OpenSim: open-source software to create and analyze dynamic simulations of movement."

[2] The AnyBody Modeling System. Aalborg, Denmark: AnyBody Technology, 2015.

[3] Au, S.K., Bonato, P. & Herr, H. (2005) "An EMG position-controlled system for an active ankle-foot prosthesis: an initial experimental study." *IEEE International Conference on Rehabilitation Robotics* 375-379.

[4] Matthew, R.P. et al. (2016) "Generating physically realistic kinematic and dynamic models from small data sets: an application for sit-to-stand actions." *International Conference of the IEEE Engineering in Medicine and Biology Society*.

[5] Gordon, A.M., Huxley, A.F., & Julian, F.J. (1966) "The variation in isometric tension with sarcomere length in vertebrate muscle fibers." *Journal of Physiology* 185:170-192.

[6] Buchanan, T.S. et al. (2004) "Neuromusculoskeletal modeling: estimation of muscle forces and joint moments and movements from measurements of neural command." *J Appl Biomech* 20(4):367-395.

[7] MATLAB version 8.6.0. Natick, Massachusetts: The MathWorks Inc., 2015.

[8] Grant, M. & Boyd, S. (2013) CVX: Matlab software for disciplined convex programming, version 2.0 beta. `http://cvxr.com/cvx`.

[9] Khalil, W. & Dombre, E. (2004) "Numerical computation of the base parameters (Appendix 5)." *Modeling, Identification & Control of Robots*.

[10] Chaffin, D.B., Andersson, G.B.J., & Martin, B.J. (2006) "Anthropometric Data for Biomechanical Studies in Industry (Section 3.2)." *Occupational Biomechanics*.